IOP PUBLISHING MEASUREMENT SCIENCE AND TECHNOLOGY

Meas. Sci. Technol. **20** (2009) 025703 (9pp) doi:10.1088/0957-0233/20/2/025703

Frequency-dependent viscoelasticity measurement by atomic force microscopy

Nan Yang[1], Kenneth Kar Ho Wong[2], John R de Bruyn[1] and Jeffrey L Hutter[1]

[1] Department of Physics and Astronomy, The University of Western Ontario, London, ON N6A 3K7, Canada

[2] Department of Medical Biophysics, The University of Western Ontario, London, ON N6A 5C1, Canada

E-mail: nyang6@uwo.ca and jhutter@uwo.ca

Received 3 September 2008, in final form 27 October 2008
Published 30 December 2008
Online at stacks.iop.org/MST/20/025703

Abstract

We demonstrate a new technique for investigating viscoelastic properties of soft materials using the atomic force microscope. A small oscillatory voltage is added to the deflection signal of the atomic force microscope causing a vertical oscillatory sample motion. Monitoring the amplitude and phase of this motion allows determination of the viscous and elastic moduli of the sample as a function of frequency during contact imaging. This technique is applied to suspended poly(vinyl alcohol) nanofibers and poly(vinyl alcohol) hydrogels, giving results similar to those measured using traditional static methods. However, the moduli of both the fibers and the hydrogels show a significant frequency dependence. The Young's modulus of the fibers increases with frequency, while for the viscoelastic hydrogels, the storage modulus dominates the mechanical response at low frequency whereas the loss modulus dominates at high frequency.

Keywords: atomic force microscope, rheology, viscoelasticity, nanofiber, hydrogel

(Some figures in this article are in colour only in the electronic version)

1. Introduction

When subjected to small deformations, solids store energy and provide a spring-like elastic response, while liquids dissipate energy through viscous flow. More complex materials display viscoelasticity, a combination of solid and fluid-like responses which generally depends on the timescale over which the sample is probed. One way to determine viscoelastic properties is to measure the shear modulus as a function of frequency by applying a small amplitude oscillatory shear strain and measuring the resultant shear stress. This kind of experiment typically requires milliliter sample volumes and only provides information on the bulk response of the material. This method does not allow local measurement in inhomogeneous systems, and samples with lower dimensionality, such as films, nanofibers and nanoparticles cannot be probed directly.

The atomic force microscope (AFM) has been widely used to study the structure of soft and biological materials with sub-nanometer resolution [1–4]. In addition to imaging, the AFM is increasingly used to measure the local elasticity and viscoelasticity of soft samples, including bone marrow [5], gelatine [6, 7], polyacrylamide gels [8], platelets and living cells [8, 9]. The advantage of AFM measurements is that topographic images can be obtained simultaneously with the mechanical response, allowing elasticity to be correlated with local structure.

During an AFM experiment, a probe attached to a weak cantilever spring is brought into contact with the sample and the cantilever deflection is monitored as the sample is scanned laterally. In constant-force mode, the cantilever deflection is kept constant by a feedback circuit that adjusts the height of a piezoelectric scanner, on which the sample is mounted, in response to the local topography. The loading force applied to the surface of the sample can be calculated from the deflection of the cantilever and Hooke's law. A soft material will deform in response to the cantilever force, providing an opportunity to measure its mechanical properties. One common technique involves indenting the sample by translating it through a vertical ramp. The discrepancy between the known vertical

displacement and resulting cantilever deflection can be used to infer the elastic properties of the sample. We refer to this as the force-curve technique; when this technique is applied over a grid of sample positions, we call it the force-volume technique [10]. However, the effects of non-vertical motion due to sliding of the inclined cantilever along the sample surface (e.g., shear deformation and frictional effects) as well as surface adhesion can complicate the analysis. Cuenot *et al* used a resonant contact AFM technique to measure the elastic modulus of nanotubes with a small-amplitude vertical motion, allowing shear to be neglected [11]. Kos and Hurley improved the contact-resonance method by designing electronics to accurately track the resonant frequency [12]. While these methods allow measurement of the elastic modulus of the sample, they do not provide information about the viscous response. Fretigny *et al* determined the complex modulus of styrene-butadiene films by modeling the longitudinal displacement of the tip on samples in the static friction regime [13]. AFM measurements using intermittent contact mode or force modulation mode, both of which image surfaces with a cantilever oscillating at a fixed frequency, can reveal contrast in the viscoelastic properties of the sample, but their nonlinear behavior complicates the analysis [14, 15]. Krotil *et al* modulated a low frequency sinusoidal signal with a high frequency oscillation to simultaneously measure the topography, the adhesion forces, applied normal forces and elastic properties of a heterogeneous polymer surface [16]. Sahin *et al* recently designed torsional cantilever tips that allow detailed mechanical properties to be measured during intermittent contact imaging [17].

Measurement of viscoelastic properties requires that forces vary on timescales shorter than the duration of the vertical ramps used in the force-volume technique, which are usually applied at a rate of at most several Hz. Mahaffy *et al* superimposed an external oscillation at frequencies of 50–300 Hz on a much slower vertical ramp of the AFM scanner and extended the Hertz model for a spherical tip in contact with a flat surface to include a frequency-dependent complex modulus E^*. They applied this approach to polymer gels and biological cells [8].

In this paper, we describe a new AFM technique for investigating frequency-dependent viscoelastic properties, which we demonstrate on poly(vinyl alcohol) (PVA) nanofibers and hydrogels. A small oscillatory voltage with an amplitude of approximately 0.1 V was added to the feedback loop of the AFM during contact mode operation and images were generated according to the resultant motion of the sample. The frequency-dependent viscoelastic modulus can be determined by analyzing the amplitude and phase of this motion relative to the external oscillation. This technique differs from that of Mahaffy *et al* in that their oscillation was added to the sample stage during force ramps whereas ours is added to the AFM's feedback loop during contact mode imaging. The validity of this method was verified by comparing the results with those from traditional static methods. The main advantages of this method are that the mechanical measurements can be done in an imaging mode, rather than extracted by post-processing of force-volume data, and that the position and frequency dependence of the viscoelasticity can be easily measured. Moreover, this method can be easily and inexpensively retrofitted to existing AFM equipment.

2. Materials and methods

2.1. Sample preparation

The PVA fibers studied in this work were made by an electrospinning technique described previously [18]. PVA with a molecular weight of 89 000–98 000 g mol^{-1} (99+% hydrolyzed) was purchased as a powder from Sigma–Aldrich Co. An electrospinning solution consisting of 8.5 wt% PVA in a solvent of 80% distilled water and 20% ethanol was used. A randomly oriented non-woven fabric of nanofibers was produced by a horizontal electrospinning setup with an aluminum collector stage under a 1.5 kV cm^{-1} electric field, a distance of 15 cm to the target and a 0.2 ml h^{-1} solution-feeding rate. Details have been published elsewhere [19]. The length and diameter of the fibers were characterized by imaging with a Leo 1530 (LEO Electron Microscopy Ltd) scanning electron microscope.

PVA hydrogels were produced by cyclic freezing and thawing of an aqueous PVA solution [20]. The same PVA powder as above was dissolved to a concentration of 12 wt% in milli-Q water at a temperature of 90 °C under reflux and stirred for 3 h. After cooling, the solution was used to fill aluminum molds 8 cm square by 0.5 mm thick. The molds were sealed and immersed in a temperature controlled bath which contained a 50% mixture of ethylene glycol in water. The PVA in the molds was subjected to up to 6 thermal cycles, each of which involved cooling from 20 °C to −20 °C at a rate of 0.12 °C min^{-1}, staying at −20 °C for 2 h, then warming to 20 °C at 0.12 °C min^{-1}. Hydrogel films were removed from the molds, cut into small pieces and stored in distilled water until required for the AFM measurements.

2.2. Atomic force microscopy

A Multimode atomic force microscope with a Nanoscope IIIa controller (Veeco Instruments) was used for all AFM measurements. The PVA fibers were imaged in air, while the hydrogels were imaged in water using a fluid cell (Veeco Instruments). Si_3N_4 cantilevers with nominal spring constants of 0.32 N m^{-1} (NP-S cantilever C, Veeco Instruments) were used for fiber imaging and cantilevers with spring constants of 0.12 N m^{-1} (NP-S cantilever B) were used for hydrogel experiments. An 8 μm diameter polystyrene microsphere was glued under the tip of the cantilever for hydrogel imaging in order to make a spherical contact with the sample surface. The force constants of the cantilevers were calibrated using the thermal noise method [21].

As described below, we modified the AFM feedback loop by adding a small sinusoidal voltage to the vertical deflection signal of the AFM. A digital lock-in amplifier implemented in LabView (National Instruments) was used to detect the amplitude and phase of the oscillation of the cantilever deflection relative to the external oscillation. The output of

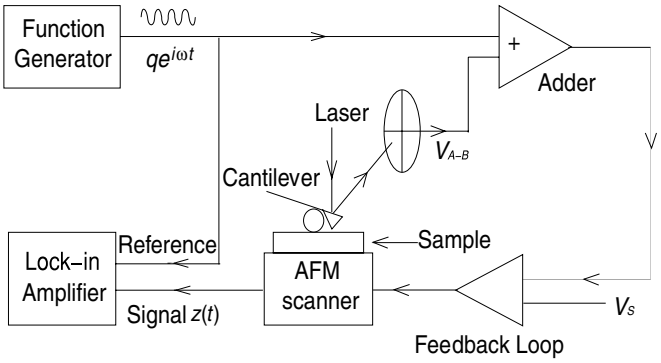

Figure 1. Schematic showing the basic operation of the AFM in contact mode, with modifications described in the text. The adder consists of a standard inverting adder followed by a unity-gain inverting amplifier.

the lock-in amplifier was input back to the AFM through a signal access monitor to generate images simultaneous with the usual topographical image.

2.3. Oscillatory method

The AFM used senses cantilever deflection with a four-quadrant photodetector that detects the position of a laser beam reflected from the cantilever, producing a signal termed V_{A-B}. In contact mode, the AFM feedback electronics causes a piezoelectric scanner to move the sample vertically so as to maintain V_{A-B} at a constant setpoint value V_s. We modified the AFM feedback loop to add a small oscillatory voltage of angular frequency ω and amplitude q to the deflection signal as shown schematically in figure 1. This results in a compensatory vertical oscillation of the sample platform, which in turn causes the cantilever to oscillate while maintaining V_{A-B} constant. The amplitude of the sample platform motion is determined by the added signal, the detector calibration and the sample properties. For instance, if the sample is perfectly rigid, the amplitude of the cantilever oscillation would be equal to that of the scanner oscillation, and if the gain of the feedback loop is high enough, the two motions would be in phase. For a material with a finite elastic modulus, the oscillation amplitude of the cantilever deflection will be smaller than that of the scanner due to deformation of the sample surface. If the sample is viscoelastic, the viscous component of its response will cause the cantilever deflection to be out of phase with the motion of the scanner. A voltage signal $z(t)$ proportional to the vertical position of the AFM scanner is available via a signal access monitor; we used a lock-in amplifier implemented using LabView software to measure its amplitude and phase. Below, we model this system using a viscoelastic extension of the standard Hertz theory [8, 22, 23].

In the absence of any added external oscillation, the vertical deflection signal is given by

$$V_{A-B} = V_0 + \frac{y(t)}{S}, \tag{1}$$

where V_0 is a constant, $y(t)$ is the deflection of the cantilever and S is the cantilever sensitivity. When the tip is in contact with the sample, $y(t)$ depends on the vertical position of the scanner $z(t)$, the unperturbed sample thickness h_0 and the deformation $\delta(t)$ of the sample due to the AFM tip,

$$y(t) = y_0 + z(t) + h_0 - \delta(t), \tag{2}$$

where y_0 is a constant and we have defined $\delta(t)$ to be positive downward and all other quantities to be positive upward.

The function of the AFM feedback electronics is to maintain V_{A-B} equal to a given setpoint voltage V_s by adjusting the vertical position $z(t)$ of the scanner. We can thus write

$$V_s = V_0 + \frac{z(t) - \delta(t)}{S}, \tag{3}$$

where for simplicity we have defined $y_0 = 0$ and $h_0 = 0$. For equation (3) to be true at all times, we must have $V_0 = V_s$ and $\delta(t) = z(t)$; in other words, the scanner position simply adjusts to compensate for the deformation of the sample, keeping the cantilever deflection $y(t)$ constant.

If we now add an oscillatory voltage $q\,\mathrm{e}^{\mathrm{i}\omega t}$ to V_{A-B}, the feedback attempts to maintain

$$V_s = V_0 + \frac{z(t) - \delta(t)}{S} + q\,\mathrm{e}^{\mathrm{i}\omega t} \tag{4}$$

constant. From the time-dependent terms we get

$$z(t) = \delta(t) - qS\,\mathrm{e}^{\mathrm{i}\omega t}, \tag{5}$$

showing that the oscillatory motion of the scanner depends on both the externally applied voltage and the deformation of the material surface $\delta(t)$.

We first consider applying this method to a perfectly rigid sample, for which there is no surface deformation. In this case $\delta(t) = 0$, and from equation (5) the position of the scanner is given by

$$z(t) = qS\,\mathrm{e}^{\mathrm{i}(\omega t + \pi)}. \tag{6}$$

Here the scanner position oscillates with an amplitude qS and a phase of π relative to the added oscillation.

We now consider a suspended elastic fiber of length L subjected to a downward force F by the AFM tip, as shown in figure 2. From standard beam deflection theory [24], the deformation of the fiber at the location of the tip is given by [10]

$$\delta = \frac{F}{3IE}\left[\frac{x(L-x)}{L}\right]^3 = CF, \tag{7}$$

where x is the position along the fiber at which the force is applied, $I = \pi D^4/64$ is the area moment of inertia of a cylindrical fiber of diameter D, E its Young's modulus and $C = [x(L-x)/L]^3/3IE$ its compliance.

The loading force F exerted by the AFM tip on the fiber is due to the bending of the cantilever. By Hooke's law, we

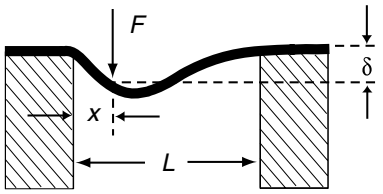

Figure 2. Illustration of the deformation of a fiber clamped to supports a distance L apart while subject to a vertical force F applied at a distance x from one end of the fiber.

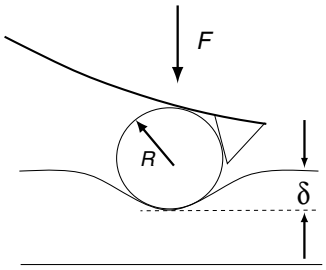

Figure 3. Deformation of a soft surface depressed by a rigid sphere of radius R, which is glued under an AFM tip. δ is the deformation of the surface as a result of the applied force F.

have $F = ky(t)$, where k is the cantilever spring constant and F is downward. Equation (2) then yields

$$y(t) = z(t) - CF = z(t) - kCy(t). \tag{8}$$

Solving for $y(t)$, we find

$$y(t) = \frac{z(t)}{1 + Ck}, \tag{9}$$

which upon substitution into equation (5) yields

$$z(t) = qS(1 + Ck)\,\mathrm{e}^{\mathrm{i}(\omega t + \pi)}. \tag{10}$$

Thus for this case the oscillatory response of the scanner has an amplitude $z_0 = qS(1 + Ck)$ and a phase of π relative to the added voltage. C depends on the point of application of the force, so the amplitude will vary with position x along the fiber, but the phase will remain constant if viscous effects can be neglected. Since the functional form of C is known, measurements of z_0 as a function of x can be used to determine the Young's modulus E of the fiber.

Finally, we consider the case in which the AFM tip is in contact with a viscoelastic surface. In this case, the compliance of the material is in general a function of the loading force. In our experiments on hydrogel films, we use a spherical probe as shown in figure 3 and model the deformation of the sample in terms of Hertz theory [22, 23]:

$$F = \tfrac{4}{3} K R^{1/2} \delta^{3/2} = \alpha \delta^{3/2}. \tag{11}$$

Here $K = E/(1 - \nu^2)$, ν is the Poisson's ratio of the sample, R is the probe radius and $\alpha = 4KR^{1/2}/3$. K will in general be complex, reflecting both viscous and elastic contributions to the complex modulus E, and will be a function of frequency ω. In using equation (11) we have assumed that the spherical probe itself does not deform, and that δ is much smaller than both the sample thickness and the spherical probe radius [8, 22, 25]. These assumptions are well satisfied in our experiments.

To measure the frequency-dependent complex modulus of the material, a small oscillatory force $F_1(t)$ with angular frequency ω can be applied around an average loading force F_0. This leads to an oscillatory deformation of the surface $\delta_1(t)$ about the initial deformation δ_0. Expanding equation (11) in a Taylor series about δ_0, we get [8, 23]

$$F = F_0 + F_1(t) = \alpha(0)\delta_0^{3/2} + \tfrac{3}{2}\alpha(\omega)\delta_0^{1/2}\delta_1(t). \tag{12}$$

Here $\alpha(0)$ is calculated using $E(0)$, the zero-frequency value of the complex modulus, and $\alpha(\omega)$ using $E(\omega)$ evaluated at the frequency of the oscillating applied force. As above, F is related to the cantilever deflection $y(t)$ by Hooke's law. We write $y(t) = y_0 + y_1(t)$, where y_0 here is the deflection corresponding to the mean deformation δ_0, and substitute $F = ky(t)$ into equation (12) to obtain a relationship between the deformation and the cantilever deflection,

$$\delta_0 = \left[\frac{ky_0}{\alpha(0)}\right]^{2/3}, \tag{13}$$

and

$$\delta_1(t) = \frac{2ky_1(t)}{3\alpha(\omega)\delta_0^{1/2}}. \tag{14}$$

Substituting these results into equation (2) and solving for $y_1(t)$, we find

$$y_1(t) = \left[1 + \frac{2k}{3\alpha(\omega)\delta_0^{1/2}}\right]^{-1} z_1(t), \tag{15}$$

where $z_1(t)$ is the time-dependent part of the scanner position $z(t)$. Using equations (4) and (5), we find

$$z_1(t) = -qS\left[1 + \frac{2k}{3\alpha(\omega)\delta_0^{1/2}}\right]\mathrm{e}^{\mathrm{i}\omega t} \tag{16}$$

$$= \tilde{z}\,\mathrm{e}^{\mathrm{i}(\omega t + \pi - \phi)}, \tag{17}$$

where $\tilde{z}$ is the amplitude of the response and ϕ is the contribution to the phase shift due to the frequency-dependent complex modulus $E(\omega)$.

In practice, it is difficult to measure ϕ accurately because of additional phase shifts that may exist in the electronics and viscous effects due to the cantilever itself as it moves through a viscous medium. We therefore take the ratio ρ of $z_1(t)$ measured for the viscoelastic sample (equation (17)) to the response measured for a rigid substrate (equation (6)) with other experimental parameters (cantilever, fluid, etc.) held constant. Any additional phase shifts (e.g., due to the circuit and cables) will be the same for both measurements and so cancel out, so the ratio is

$$\rho = 1 + \frac{2k}{3\alpha(\omega)\delta_0^{1/2}} \tag{18}$$

$$= 1 + \frac{k}{2R^{1/2}[E(\omega)/(1-\nu^2)]\delta_0^{1/2}}. \tag{19}$$

Since k and R are constants determined by the experimental apparatus and δ_0 can be calculated from the setpoint and force curves obtained on the sample surface, this approach allows us to determine the value of $K(\omega) = E(\omega)/(1-\nu^2)$ as a function of the frequency of the applied oscillation.

2.4. Static method

The Young's modulus of suspended fibers can be measured with the AFM using the force-volume (FV) technique described in [10]. Briefly, force curves are obtained by measuring the cantilever deflection resulting from a known

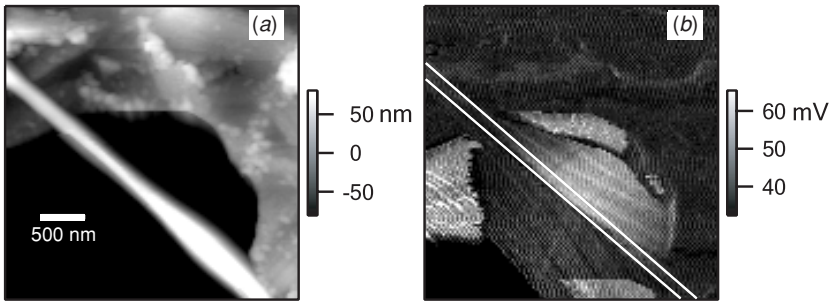

Figure 4. AFM images for a suspended fiber: (*a*) height image; (*b*) oscillation amplitude image. The fiber had a suspended length of 2.79 μm and a diameter of 124 nm. The lines in (*b*) indicate the range over which the data were analyzed.

vertical ramp of the sample platform at a rate up to several Hz. Since the slope of the force curve when the tip is in contact with the fiber depends on the sample compliance, the Young's modulus of the beam can be determined by modeling the shape of the curve. As discussed above, the loading force on a suspended fiber is $F = ky(t)$, and the deformation due to this force is given by equation (7). The deflection of the cantilever $y(t) = z(t) - \delta$ becomes

$$y(t) = z(t)\left[1 + \frac{k}{3EI}\left(\frac{x(L-x)}{L}\right)^3\right]^{-1}, \tag{20}$$

so the measured slope of the contact portion of the force curve is

$$\frac{\mathrm{d}y}{\mathrm{d}z} = \left[1 + \frac{k}{3EI}\left(\frac{x(L-x)}{L}\right)^3\right]^{-1}. \tag{21}$$

In an AFM experiment, a force-volume image of a region containing the fiber is collected. The theoretical slope is $\mathrm{d}y/\mathrm{d}z = 1$ for points on the rigid substrate, while the slope along the suspended portion of the fiber will be a function of the distance x from the edge of the substrate. These slopes, normalized by the mean slope on the substrate, are fitted to equation (21) to determine the Young's modulus of the fiber.

When this technique is applied to a soft film such as a hydrogel, the force curves are not linear. In this case, during the contact portion of a force curve ramp the cantilever deflection is

$$y - y_0 = z - z_c - \delta, \tag{22}$$

where z_c is the contact point, y_0 is the initial cantilever deflection and δ is given by equation (11). Thus

$$z - z_c = \left[\frac{3k(1-\nu^2)}{4ER^{1/2}}\right]^{2/3}(y-y_0)^{2/3} + (y-y_0). \tag{23}$$

This is a third-order polynomial equation of the form

$$x^3 + bx^2 + d = 0 \tag{24}$$

in the variable $x \equiv (y-y_0)^{1/3}$, with $b = [3k(1-\nu^2)/(4ER^{1/2})]^{2/3}$ and $d = z_c - z$. If the tip is in contact with the sample surface, d is negative and the deflection $y - y_0$ is positive. Depending on the sign of the discriminant

$$\Delta = \frac{d^2}{4} + \frac{db^3}{27}, \tag{25}$$

the desired solution is

$$x = s_+ + s_- - \frac{b}{3}, \tag{26}$$

where

$$s_\pm = \begin{cases} [-108d - 8b^3 \pm 12\sqrt{3d(27d+4b^3)}]^{1/3}/6 & \text{for } \Delta \geqslant 0 \\ \dfrac{b}{3}\cos\dfrac{\theta}{3} & \text{for } \Delta < 0 \end{cases} \tag{27}$$

and $\theta = \arccos(-(27d + 2b^3)/2b^3)$. By fitting the measured values of $y - y_0$ as a function of $z_c - z$ to equation (26), we can extract the static Young's modulus E.

3. Results and discussion

3.1. PVA nanofibers

We first used our oscillatory technique to measure the Young's modulus of suspended PVA fibers. The PVA fibers were deposited on a TEM grid to suspend them across square holes with 7.5 μm sides. The suspended length and average diameter of the fiber were measured by SEM, and samples were imaged both before and after the experiment to ensure the fiber had not moved during the experiment. Figure 4 shows AFM images of (*a*) height and (*b*) oscillation amplitude (measured by the lock-in amplifier) for a fiber of suspended length 2.79 μm and diameter 124 nm. In this example, the frequency of the sinusoidal voltage added to the AFM feedback was 500 Hz. The phase of the fiber oscillation was constant during imaging, as expected from equation (10) for a purely elastic fiber. Thus viscous effects are negligible, so we studied the elastic modulus of the fiber by analyzing the amplitude of the response.

The oscillation amplitude image of figure 4(*b*) shows a complicated structure. The amplitude on the supported portion of the fiber is the same as that on the bare substrate, where there is no fiber, as expected. Far from the suspended portion of the fiber (lower left corner) the sample lies beyond the vertical range of the scanner, resulting in no signal. In regions near the suspended fiber or the edge of the pit, it is possible for the side of the tip, a square pyramid 4 μm across at the base, rather than its apex, to contact the sample. This results in poor tracking and noisy features. Such effects were seen in the height image as well, but the gray-scale in figure 4(*a*) was chosen to avoid these features for clarity. Moreover, contact with the side of the tip produces deflection forces in significantly different

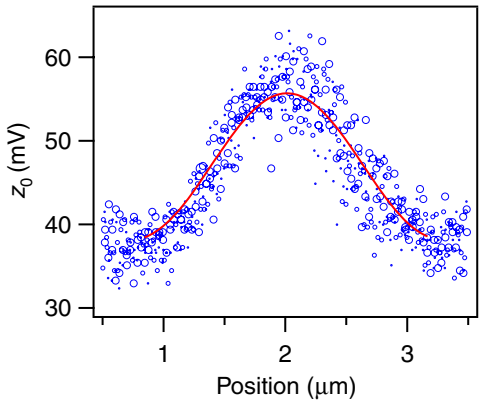

Figure 5. Oscillation amplitude z_0 (circles) as a function of position along the suspended fiber shown in figure 4. The sizes of the circles indicate the distance from the midline of the fitting range for each point: the larger the size, the closer to the midline. The solid curve is a fit to equation (10).

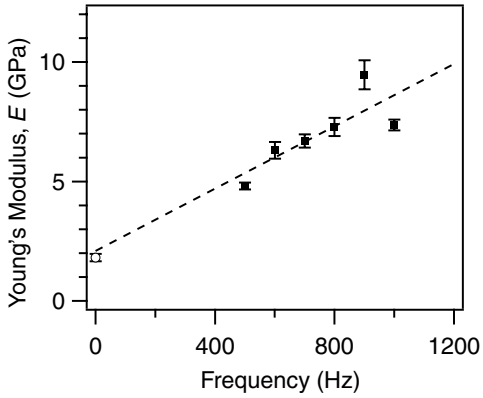

Figure 6. Young's modulus of a PVA fiber as a function of frequency. Solid squares: Young's modulus determined by the oscillatory method. Open circle: the low-frequency Young's modulus of the same fiber measured by the force-volume technique. The dashed line is a fit to the oscillatory data only.

directions from the vertical direction assumed by our model; thus, these regions are of no use for our analysis. The lines in figure 4(*b*) indicate a range of locations near the midline of the fiber, where our model can be applied. It can be seen that the amplitude is larger in the middle of the suspended part of the fiber, as expected from equations (7) and (10).

If the gain of the AFM feedback loop is not high enough, the scanner will not be able to keep up with the external oscillation, leading to an apparent value of the Young's modulus larger than the true value. We performed measurements with a range of gain settings to verify that the gain we used was high enough that the amplitude of the response of the rigid substrate was independent of the gain. This is much the same as the way in which gain settings are chosen in conventional contact imaging to ensure that the specific settings used do not influence the height information.

To extract the Young's modulus E, we fit the oscillation amplitude z_0 from all pixels within the range shown in figure 4(*b*) to the model, equation (10). The results are shown in figure 5. The range covered by the fit line corresponds to the suspended length of the fiber. The value of E obtained from the fit is 4.37 ± 0.06 GPa, where the uncertainty reflects the statistical uncertainty in the fit. The uncertainty in the cantilever spring constant is not included, since it introduces a systematic effect which is the same for all measurements made with the same cantilever.

We measured the Young's modulus of a PVA fiber as a function of frequency from 500 to 1000 Hz, where the maximum frequency is determined by the finite bandwidth of our modified electronics and the minimum is determined by the minimum scan rate of the AFM. The time constant of the lock-in amplifier was set at 10 times the oscillation period and so was between 10 ms and 20 ms. Since the dwell time of the AFM was about 78 ms pixel^{-1}, this was long enough to give a stable response at each pixel of the AFM image. Figure 6 shows the results for this fiber, which had a suspended length of 4.15 μm and diameter of 179 nm. It is seen that the modulus increases by a factor of two over the frequency range studied, highlighting the importance of frequency-dependent measurements.

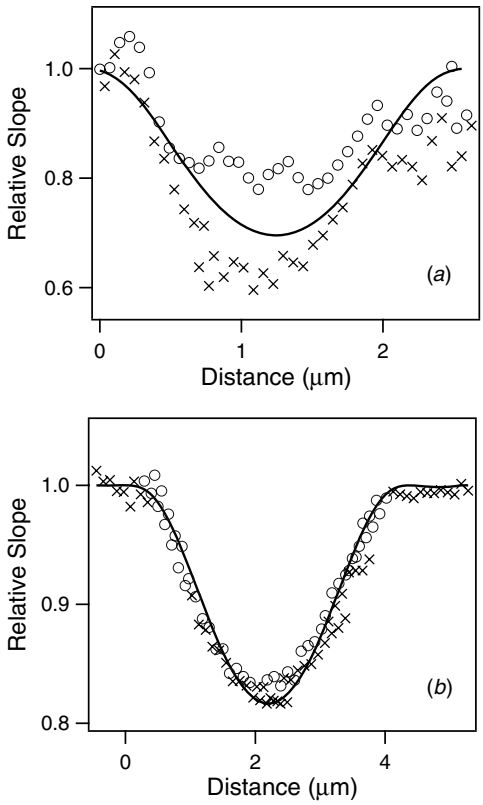

Figure 7. Relative slope as a function of distance along suspended fibers for (*a*) the fiber as shown in figure 4, and (*b*) a different fiber in which data more closely follow a single curve. The two series are points from above (circles) and below (crosses) the fibers, relative to their height images. The lines are fits of the relative slopes to equation (21).

We also performed force-volume measurements to determine the zero-frequency Young's modulus of the same fibers for comparison with our new method. The relative slope as a function of position for the fiber shown in figure 4 is plotted in figure 7(*a*). In this case the data split into two series, one above and one below the fitted curve. This is because the diameter of the fiber is small compared to the size of the tip.

As a result, very few force curves are measured precisely on the midline of the fiber. Instead, many of the points in the FV data represent contact between the fiber and the sides of the pyramidal tip, resulting in off-center loading. In order to demonstrate this, figure 7(*a*) labels all points acquired above the midline of the fiber as circles, and those acquired below the fibers as crosses. The nearly perfect division of points verifies the dependence on the precise position of the measurement relative to the fiber.

The origin of the different slopes is easily understood: for instance, if the fiber contacts the side of the tip furthest from the cantilever base, as is the case for points measured above the fiber in figure 4, it gives rise to a torque that decreases the cantilever deflection from that which would occur for a purely vertical contact force. For the same reason, a larger vertical oscillation is needed to compensate for the added signal in the oscillatory method, explaining the fact that amplitudes measured above the fiber are higher than those measured below in figure 4(*b*).

Figure 7(*b*) shows the relative slopes for a different PVA fiber with length 3.70 μm and diameter 114 nm. In this case a much smaller splitting is seen, presumably because the data were taken closer to the midline. Effects of the tip position are evident in the oscillatory method as well, but the higher pixel density always results in a scatter of points similar to that seen in figure 5, providing a realistic assessment of the uncertainties inherent in this technique. The value of the Young's modulus obtained by fitting the data in figure 7(*a*) is 4.6 $\pm$ 0.3 GPa. The quoted uncertainty again does not include the uncertainty in the cantilever calibration or in the fiber dimensions, since the same cantilever and fiber were used for both oscillatory and static measurements. For the fiber tested in figure 6, the zero-frequency Young's modulus (open circle in figure 6) was 1.8 $\pm$ 0.2 GPa, in agreement with the linear extrapolation of the oscillatory data to an intercept of 2.1 $\pm$ 1.8 GPa.

To test the reproducibility of the oscillatory technique, we measured the Young's modulus of nine fibers at a frequency of 500 Hz and compared these values to those obtained by the FV method for the same fibers. Since the Young's modulus varies between fibers, we examined the ratio between the values determined from the two techniques, which we found to be 1.37 $\pm$ 0.16. This agrees with our finding that the Young's modulus increases with frequency, while the magnitude of the uncertainty provides a measure of the consistency of the technique.

3.2. PVA hydrogels

We also used the oscillatory technique to measure the viscoelastic properties of PVA hydrogels. PVA hydrogels of thickness 0.5 mm were attached to silicon plates using cyanoacrylate glue. AFM measurements were made in a fluid cell with a glass cantilever holder. As above, oscillatory experiments were performed in contact mode with a small sinusoidal voltage added to the feedback loop of the AFM. In order to simplify the data analysis, each measurement was done at a single point on the surface of the sample by setting the imaging size to zero. We performed measurements at three

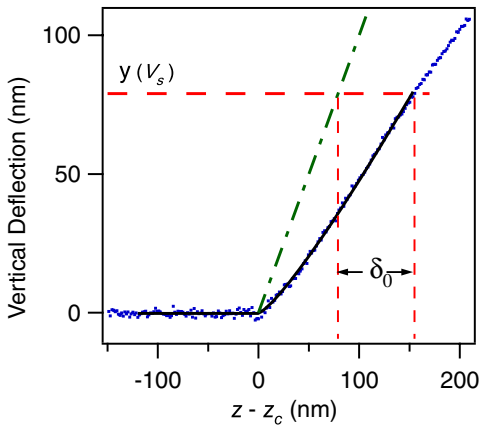

Figure 8. Force curve used to determine δ_0 for the oscillatory method. Dots: measured force curve for a 4-cycle PVA hydrogel. Dot-dashed line: theoretical force curve on a silicon plate. Solid line: a fit to equation (23) used to determine the static Young's modulus of the PVA hydrogel.

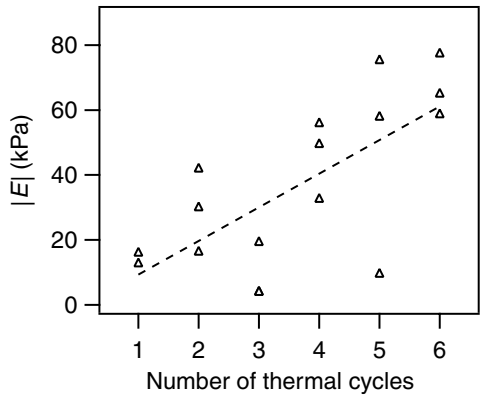

Figure 9. Magnitude of the complex modulus measured by the oscillatory technique at 50 Hz for PVA hydrogels subjected to a varying number of thermal cycles during preparation. $|E|$ was measured at three locations on each of six samples. The dashed line is a linear fit to the data points as a function of the number of thermal cycles.

different locations on each sample. Figure 8 shows how the mean deformation δ_0 was determined. The hydrogel sample was mounted on a rigid silicon plate and force curves were recorded on the hydrogel and on a base portion of the silicon plate. The difference in $z - z_c$ between the two force curves at the setpoint V_s is equal to the deformation δ_0. The exact value of V_s is unimportant as long as the deflection of the cantilever remains in the linear regime. For the force curve in figure 8, V_s is about 1.65 V and δ_0 is about 95 nm. The force constant of the cantilever here is 0.093 N m^{-1} and its sensitivity is about 47 nm V^{-1}.

Figure 9 summarizes the results of measurements made at 50 Hz on hydrogels prepared with different numbers of thermal cycles. The moduli were found to vary from point to point on a given sample by substantially more than the experimental uncertainties, confirming earlier reports that the PVA hydrogel surface is nonuniform [20]. The linear fit indicates that although there is a wide variability, the average modulus increases with the number of cycles.

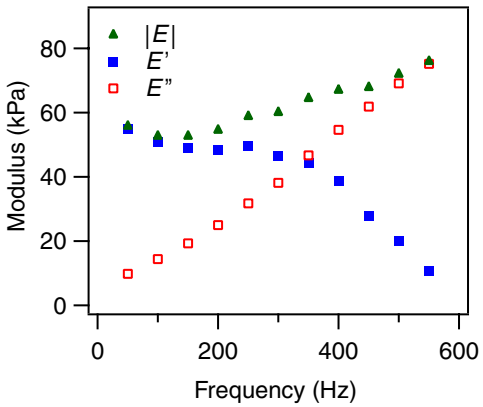

Figure 10. Complex modulus of a PVA hydrogel (four thermal cycles) as a function of frequency. E' is the storage modulus (real part); E'' is the loss modulus (imaginary part); $|E| = (E'^2 + E''^2)^{\frac{1}{2}}$ is the magnitude of the complex modulus.

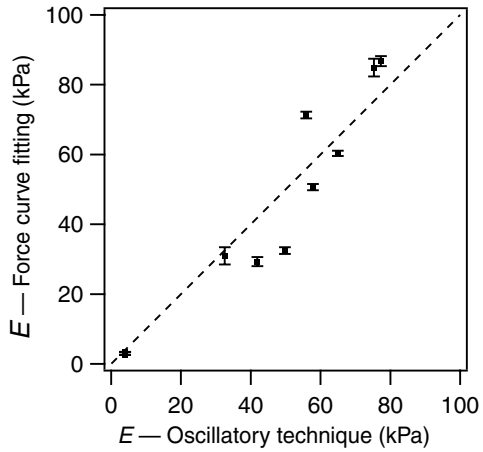

Figure 11. Comparison of moduli determined by the static force curve fitting technique and the oscillatory technique at 50 Hz. The dashed line corresponds to equality of the values determined from the two techniques.

Figure 10 shows the dependence on frequency of the complex modulus of a PVA hydrogel subjected to four thermal cycles during preparation. The magnitude of the modulus increases with frequency from a low frequency value of about 55 kPa, which is consistent with bulk results reported elsewhere [20]. The storage modulus E', the real part of the complex modulus, dominates the mechanical response at low frequency while the loss modulus E'', the imaginary part, dominates at high frequency. We interpret this as an indication that viscous effects due to motion of the polymer chains in the fluid within the hydrogel become increasingly important as the frequency increases. Note that the main source of uncertainty in the moduli comes from the determination of the mean deformation δ_0. In our instrument, variation in the deflection signal due to, for example, mechanical creep or electrical drift can result in uncertainties of up to 5% in δ_0.

We also compared the magnitude of the complex modulus of the PVA hydrogels to the Young's modulus measured by fitting the force curves to equation (23). Since the viscoelastic properties of the hydrogels vary across the sample, force curves were measured before and after each oscillatory measurement, at the same location on the hydrogel sample and with the same experimental parameters, to allow for a meaningful comparison. One example is shown in figure 8, for which the fit indicates a Young's modulus of 71± 1 kPa, which is within the range of $|E|$ determined by the oscillatory method for the four-cycle hydrogel (see figure 10). Figure 11 compares the moduli of hydrogel samples measured from the force curves at a 1 Hz ramp rate with those measured by the oscillatory technique at 50 Hz. The data points are taken from various locations on each of the hydrogel samples. The ratio of the modulus obtained from the oscillatory technique to that from the static technique is 1.14 ± 0.08, indicating that, on average, the modulus at 50 Hz is slightly larger than that at 0 Hz.

4. Conclusion

We have developed a new technique for measuring the viscoelastic response of soft materials using atomic force microscopy. This technique was implemented by using an external circuit to add an oscillatory voltage to the feedback loop of the AFM. The response was measured using a lock-in amplifier and viewed as an image alongside the usual AFM topography image. The main advantages of this technique over conventional AFM-based techniques for measuring mechanical properties are that it can be done in imaging mode, simplifying the setup and analysis, and the excitation frequency can be easily varied, allowing viscoelastic properties to be determined as a function of frequency. The validity of this method was confirmed by comparing results for electrospun PVA nanofibers and physically cross-linked PVA hydrogels with those measured by the static techniques. The Young's modulus of the nanofibers increased linearly with frequency; extrapolating the data to zero frequency gave a static Young's modulus in good agreement with that measured with the FV method. This shows that static measurements are not sufficient to describe the mechanical properties of PVA nanofibers. Viscoelastic effects were evident in the PVA hydrogels. Our results for the frequency dependence of the complex modulus show that the storage modulus dominates the viscoelastic response of these materials at low frequency, while the loss modulus dominates at high frequency.

Acknowledgment

This work was supported by the Natural Sciences and Engineering Research Council of Canada (NSERC).

References

[1] Drake B, Prater C B, Weisenhorn A L, Gould S A C, Albrecht T R, Quate C F, Channell D S, Hansma H G and Hansma P K 1989 Imaging crystals, polymers, and processes in water with the atomic force microscope *Science* **243** 1586–9

[2] Henderson E, Haydon P G and Sakaguchi D S 1992 Atomic filament dynamics in living glial cells imaged by atomic force microscope *Science* **257** 1944–6

[3] Henderson R M and Oberleithner H 2000 Pushing, pulling, dragging, and vibrating renal epithelia by using atomic force microscopy *Am. J. Physiol. Renal Physiol.* **278** 689–701

[4] Kasas S, Thomson N H, Smith B L, Hansma P K, Mikossy J and Hansma H G 1997 Biological applications of the AFM: from single molecules to organs *Int. J. Img. Sys. Tech.* **8** 151–61
[5] Tao N J, Lindsay S M and Lees S 1992 Measuring the microelastic properties of biological material *Biophys. J.* **63** 1165–9
[6] Radmacher M, Fritz M and Hansma P K 1995 Imaging soft samples with the atomic force microscope: gelatin in water and propanol *Biophys. J.* **69** 264–70
[7] Domke J and Radmacher M 1998 Measuring the elastic properties of thin polymer films with the atomic force microscope *Langmuir* **14** 3320–5
[8] Mahaffy R E, Shih C K, MacKintosh F C and Käs J 2000 Scanning probe-based frequency-dependent microrheology of polymer gels and biological cells *Phys. Rev. Lett.* **85** 880–3
[9] Radmacher M, Fritz M, Kacher C M, Cleveland J P and Hansma P K 1996 Measuring the viscoelastic properties of human platelets with the atomic force microscope *Biophys. J.* **70** 556–67
[10] Guhados G, Wan W K and Hutter J L 2005 Measurement of the elastic modulus of single bacterial cellulose fibers using atomic force microscopy *Langmuir* **21** 6642–6
[11] Cuenot S, Frétigny C, Dmeoustier-Champagne S and Nysten B 2003 Measurement of elastic modulus of nanotubes by resonant contact atomic force microscopy *J. Appl. Phys.* **93** 5650–5
[12] Kos A B and Hurley D C 2008 Nanomechanical mapping with resonance tracking scanned probe microscope *Meas. Sci. Technol.* **19** 015504
[13] Fretigny C, Basire C and Granier V 1997 Determination of complex modulus by atomic force microscopy *J. Appl. Phys.* **82** 43–8
[14] Nony L, Boisgard R and Aimé J P 1999 Nonlinear dynamical properties of an oscillating tip-cantilever system in the tapping mode *J. Chem. Phys.* **111** 1615–27
[15] Lee S L, Howell S W, Raman A and Reifenberger R 2002 Nonlinear dynamics of microcantilever in tapping mode atomic force microscopy: a comparison between theory and experiment *Phys. Rev.* B **66** 115409
[16] Krotil H U, Stifter T and Marti O 2000 Concurrent measurement of adhesive and elastic surface properties with a new modulation technique for scanning force microscopy *Rev. Sci. Instrum.* **71** 2765–71
[17] Sahin O, Magonov S, Su C, Quate C F and Slogaard O 2007 An atomic force microscope tip designed to measure time-varying nanomechanical forces *Nature Nanotechnology* **2** 507–14
[18] Frenot A and Chronakis I S 2003 Polymer nanofibers assembled by electrospinning *Curr. Opin. Colloid Interface Sci.* **8** 64–75
[19] Wong K H, Zinke-Allmang M and Wan W K 2006 N^+ surface doping on nanoscale polymer fabrics via ion implantation *Nucl. Instrum. Methods Phys. Res.* B **249** 362–5
[20] Millon L E, Nieh M P, Hutter J L and Wan W K 2007 SANS characterization of an anisotropic poly(vinyl alcohol) hydrogel with vascular applications *Macromolecules* **40** 3655–62
[21] Hutter J L and Bechhoefer J 1993 Calibration of atomic-force microscope tips *Rev. Sci. Instrum.* **64** 1868–73
[22] Sneddon I N 1965 The relation between load and penetration and the axiymmetric Boussinesq problem for a punch of arbitrary profile *Int. J. Eng. Sci.* **3** 47–57
[23] Johnson K L, Kendall K and Roberts A D 1971 Surface energy and the contact of elastic solids *Proc. R. Soc.* A **324** 301–13
[24] Timoshenko S and Gere J M 1997 *Mechanics of Materials* (Boston: PWS Publishing)
[25] Mahaffy R E, Park S, Gerde E, Käs J and Shih C K 2004 Quantitative analysis of the viscoelastic properties of thin regions of fibroblasts using atomic force microscopy *Biophys. J.* **86** 1777–93